Preliminary study of a visible, high-resolution spectrometer for DEMO divertor survey

W. Gonzalez,[a] W. Biel,[a] Ph. Mertens,[a] M. Tokar,[a] O. Marchuk[a], F. Mourão[b], Ch. Linsmeier[a]

- *Forschungszentrum Jülich GmbH, Institut für Energie- und Klimaforschung - Plasmaphysik,*
- *52425 Jülich, Germany*
- *Instituto de Plasmas e Fusão Nuclear (IPFN), Instituto Superior Técnico, Universidade de Lisboa 1049-001 Lisboa, Portugal*

E-mail: winder.gonzalez@gmail.com

Abstract:

Developments towards DEMO Diagnostic and Control (D&C) system conceptual design are based on a subset of ITER mature diagnostic systems, whose eligibility for DEMO has been endorsed by their robustness, long lifetime expectancy and feasible remote maintenance [1]. They are devoted to ensure the machine operation in compliance with safety requirements and high availability. In particular, the evolution of divertor spectroscopic measurements on fusion experiments has demonstrated their potential as a control method for divertor protection via detachment control [2-3] (near ultraviolet, 300 – 400 nm) and monitoring of the plasma–wall interaction (visible range, 400 – 700 nm) [4]. These characteristics make this method one of the leading candidates for DEMO detachment and radiation control power. In line with the application of a system engineering approach [5], initial assessments of design and feasibility of a VIS high-resolution spectrometer for the DEMO divertor survey based on early DEMO control requirements are presented and discussed. The proposed system is located at the equatorial port and it is composed of 3 oblique lines of sights (LoS), 9 toroidal mirrors, 6 plane mirrors and 6 spectrometers examining the outer, inner and X-point divertor region, optimized for the monitoring of chord-integrated NUV/VIS signals under parallel divertor plasmas observation. The wavelengths of interest, spatial resolution and main integration issues are reported.

Keywords: DEMO diagnostic and control (D&C) system; Plasma divertor detachment; Radiation control power; Spectroscopy.

• Introduction

The demonstration fusion reactor (DEMO) in comparison to ITER will have to prove high robustness and reliability operation near technical and physics limits, over a significant pulse duration [6], with a reduced number of diagnostic systems exclusively for safety and plasma control [7]. In this context, the progress of DEMO design and R&D activities are aimed to provide an early DEMO diagnostic and

control (D&C) concept supported by a system engineering approach, based on mature technologies and reliable regimes of operation extrapolated from the future ITER experience [5].

In this phase of DEMO D&C development a prime choice of diagnostic methods applicable to the stationary burn phase of the discharge has been obtained [1]. This preliminary group of D&C systems comprises a large range of diagnostic techniques, the control function of which and integration approaches are in constant evolution. In particular the divertor plasma detachment control via the evolution of the enhanced high Balmer line intensities and Stark broadening high-resolution spectroscopy measurements represent a promising D&C system to preserve the divertor target integrity of the high heat flux densities effects (sputtering and deposition) [2].

In view of the unprecedented high levels of neutron and gamma fluxes, and fluences expected, together with high energy charge-exchange (c-x) atoms penetrating into diagnostic ports in DEMO [8], the location of any optical component considering the geometrical constrains at close proximity to the plasma will have a strong impact in terms of durability and imaging quality, determining its applicability for DEMO control. The focus of this paper is on the preliminary optical design of a high-resolution visible (VIS) spectrometer system for divertor plasma detachment detection via measurements of Balmer strong intensity emission lines and Stark broadening from hydrogen isotopes.

The paper is organized as follows. A brief description of the DEMO baseline model is given and the main geometrical constraints are discussed in connection with some criteria adopted for mirror protection; relevant to the design and implementation of an optical system for imaging of divertor plasma. As a result of this initial step, a common parametric optical layout for three optical subsystems is described as function of the image target region and wavelength range of interest, used later as input data for ZEMAX simulations. Subsequently, optics simulations results of these optical subsystems are reported and discussed. Lastly, these results are exported to a CATIA model and integrated into a simplified ITER-like diagnostic shield module (DSM) to assess its feasibility and compatibility with other diagnostics systems located at the same equatorial port (EP).

- **Divertor parallel imaging and geometrical constraints**

DEMO divertor region is an area where a strong plasma-wall interaction and high fluxes of impurity particles are expected; in consequence, to ensure the protection and long-term durability of any diagnostic component responsible for the monitoring and control of plasma detachment, its location must be protected, positioned far from the divertor region. In the first instance DEMO offers two host ports possibilities for first mirror location (M), at the vertical (VP) and equatorial port (EP); however LoS for plasma detachment observation require a parallel orientation close to the divertor targets, excluding the use of the VP as first option due to the geometrical limitations; instead, the implementation of this measurement is technically possible by integrating three optical subsystems into an EP, imaging the outer, x-point and inner divertor regions under oblique angles separately [9].

Whereas the plasma discharge evolution on DEMO and the physics models for future advanced control schemes are subjects which will be investigated in a later design stage, in this phase a flexible approach has been adopted for a complete plasma divertor observation by means of three optical systems. Nevertheless, in future, a more detailed divertor plasma shape description could suggest a reduced region of observation, leading to a reduction of the field of view and first mirror size as well.

These subsystems are devoted to transmit light in the near-UV with high-resolution for the reconstruction of high-n Balmer lines, in particular transitions ($D_{10\text{-}2}$, $D_{11\text{-}2}$, $D_{12\text{-}2}$, $D_{13\text{-}2}$) for divertor detachment control and the VIS spectrum overview for plasma impurity monitoring, splitting the light in two wavelength ranges of interest and measured by two spectrometers [2].

The DEMO EP volume is configured with a width of 1,6 m and a height of 2,8 m in toroidal and poloidal direction respectively, with an interspace average length of 6,3 m, see Fig.6. This volume has been subject of LoS analysis for parallel divertor imaging, allowing the identification of three feasible

toroidal first mirror locations (OP = OPx, OPy, OPz), see Table (1); separated from each other at a distance of ΔZ= 450 mm, with reference to the Z axis. A mechanical support structure has been conceptualized from an ITER-like diagnostic module with LoS completely contained within EP volume to prevent interferences with the vacuum vessel (VV) and other structures.

Table 1: First mirror locations at EP (M1, M2, M3)

OP	OPx [mm]	OPy [mm]	OPz [mm]
M1	13500	-500	1100
M2	13500	-500	650
M3	13500	-500	200

To ensure the protection of the optical components, a pinhole configuration has been adopted, with a breading blanket (BB) opening of = 30 mm of diameter and the inclusion of a Deuterium (D_2) flow of density n_G = 3e19m^{-3} whose visible absorption is negligible, through a labyrinth path (duct) for neutron shielding and rate erosion attenuation induced by high energy atoms (hydrogen fluxes) in optical components. In particular, first mirrors have been located at a distance of L > 1240 mm; to guarantee a large (L/) > 50 ratio and an erosion rate of h_{sp} < 8 nm/fpy [10]; In addition, the use of ducts with baffles as passive methods of protection can reduce the flux of impurities on first mirrors [11], and contribute with the intensity attenuation of the light scattered by the inner duct surface, originating from other plasma regions.

- **Meridional and sagittal plane definition**

In practice, given the parallel distances (Dtt_i) see Fig. 1, the coordinates points D1, D2 and OP according to the divertor region to be covered, and the formulation of the collinear vectors and ; under the same direction as function of the toroidal angle (), Eq.1; the minimization of the function allows the estimation of in the domain (0 < /2). This value of is used to verify the suitability of first mirror locations and opening coordinates at the Breading Blanket (BB), in agreement with the LoS conditions mentioned above, see Figure 1. To conclude, an arbitrary out-vessel D1-OP coplanar secondary optical component (SOC) coordinate point has been used (SOC = SOCx, SOCy, SOCz) to define the meridional and sagittal planes of solution for the observation of the high field side (HFS), x-point (XP) and low field side (LFS) see Fig. 1.

	Eq.1

Where:

Once the meridional and sagittal planes are defined, the optical system can be outlined and assessed through simulations oriented to optimize the image quality and resolution, but keeping in mind the tilt angle between the DEMO Z axis and the meridional plane, required to ensure the efficient use of the EP volume in poloidal orientation.

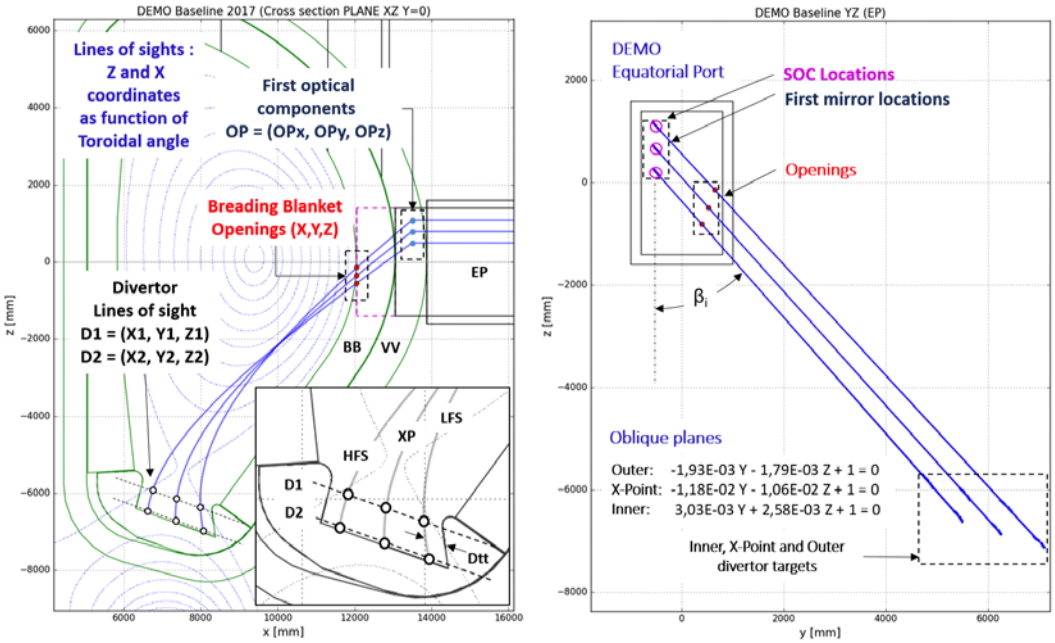

Figure 1: Divertor observation and geometrical constrains for meridional and sagittal planes.

- **Optical layout**

Based on previous results, a standard and flexible optical design has been elaborated for further improvements and analysis, see Fig. 2; first optical components are represented by toroidal mirrors (M) with symmetrical meridional and sagittal focus and ; In the meridional and sagittal planes the toroidal mirror (M) focuses light rays from the divertor plasma at the mirror (A) according to the system of equations Eq. 2; where and are the object-to-toroidal mirror and the toroidal mirror-to-mirror (A) distance, respectively. is the major radius of curvature, the minor radius of curvature of the toroidal mirror and the incident angle to the mirror in the meridional plane.

	Eq.2

Secondary optical components location are distributed along a labyrinth path within ducts with miter bend connections [12]; for a multi-configuration optical simulation, the initial conditions for some values such as radius of curvatures, optical focuses and component distances are summarized in Table 3 and Table 4. The entire system consists of three optical subsystems for HFS, XP and LFS divertor parallel observation.

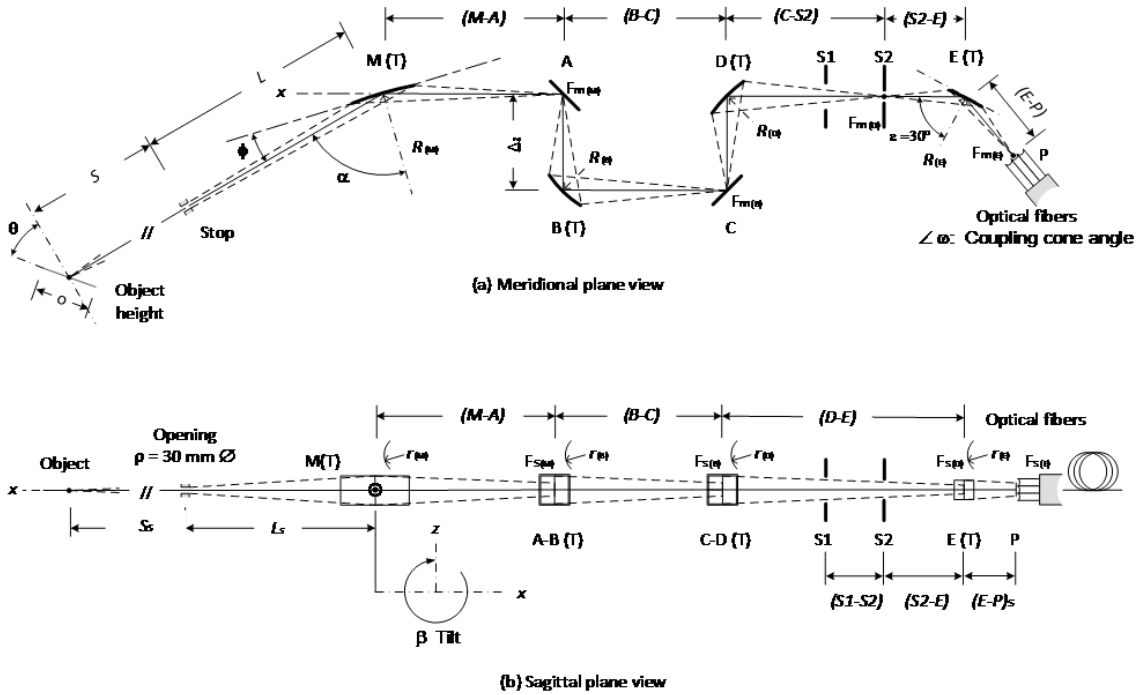

Figure 2: Common optical layout for high-resolution divertor spectroscopy, (a) Meridional plane of view and (b) Sagittal plane view.

Table 2: Optical layout (dimension properties).

Config.	S [mm]	L [mm]	M-A [mm]	ΔZ [mm]	B-C [mm]	C-S2 [mm]	S1-S2, S2-E, E-P [mm]	O [mm]	θ [Deg]	α [Deg]	β [Deg]
Outer	12366	2232	1400	450	2200	1250	500	802	26,19	65,38	42,75
X-point	11634	2148	950		3100	800		790	28,71	66,82	41,97
Inner	11071	2103	500		4000	350		763	21,41	68,59	41,42

The initial approach laid down in this design was the light propagation through the reflection of four planar mirrors (A, B, C, D) from M to S1 (Port plug), to avoid the introduction of aberrations; as a result of this test, the image resolution obtained at S2 was near to 3 mm with a beam radius around 400 mm; subsequently in order to reduce the beam radius and get a more compact optical setup, toroidal mirrors have been included at B, D and E locations for intermediate imaging, theoretical values are summarized in Table 3.

Table 3: Optical layout (Focuses and radii of curvature).

Mirror	Target	Fm=Fs [mm]	Fs' [mm]	Fm' [mm]	ϕ [Deg]	R [mm]	r [mm]
M	Outer	14598,09	1400	1400	65,38	6132,06	1064,55
	X-point	13782,30	950	950	66,82	4514,99	699,77
	Inner	13174,45	500	500	68,59	2639,72	351,63
B	Outer	450	2200	2200	45	1056,66	528,33
	X-point	450	3100	3100		1111,45	555,73
	Inner	450	4000	4000		1144,08	572,04
D	Outer	450	2250	1750	45	1012,45	530,33

	X-point	450	1800	1300		945,50	509,12
	Inner	450	1350	850		832,21	477,30
E	Outer	500	500	500	60	1000	250
	X-point	500	500	500		1000	250
	Inner	500	500	500		1000	250

The implementation of optical fibers at the location (P) see Fig.2, is subordinated to the irradiation levels and *displacements per atoms* (dpa) induced by neutrons on glass expected in this region and also the effects on the optical properties of materials to be used as transmission components [13]. Alternatively, metallic mirrors should be included, separated by a diamond window or within vacuum extensions to transport the light at safe places for optical fibers [14]. In addition to the use of diamond as hydrogen isotope barrier, diamond windows exhibits an extraordinary thermal conductivity and its transmission starts in the UV at 225 nm, covering the entire spectral range from the visible through the infrared and terahertz range up to radar frequencies.

- **ZEMAX Simulations**

A set of multi-configuration simulations have been done, using the optic layout developed in the previous section, see Fig. 2. Table 4 summarizes the field of observation coordinates simplified to represent the object high length (O) of each subsystem, see Table 2. The entrance pupil aperture (Stop) has been set to 30 mm of diameter and parallel-oriented to DEMO Z axis, with uniform apodization in VIS wavelength range within an environment at 20 C and 1 atm.

Table 4: Field of observation (Object: Divertor parallel target discretized in 9 points).

Fields	(X,Y) [mm]
1	(0,-400)
2	(0,-300)
3	(0,-200)
4	(0,-100)
5	(0,0)
6	(0,100)
7	(0,200)
8	(0,300)
9	(0,400)

Field 5 represents the centroid of the system, and reference for optimization and parallelism between the subsystems at the interspace. An initial tilted surface has been used to define the object (O) and its fields of observation; this plane is defined in terms of the tangent angle () between the normal plane to the centroid and the object, as well as the projection of it on the divertor. Toroidal surfaces have been used at locations (M, B, D, E) to reduce the beam dimensions by defining the curvature in the meridional (R) and sagittal (r) planes, Eq. 2; standard surfaces have been used for planes mirrors at locations (A, C) to ensure a free light propagation, and coordinate breaks surfaces to compensate changes of beam direction. ZEMAX 3D layout in Fig. 3 and Fig. 4, shows the integration of all subsystems in the planes ZX and YX; with an offset between them of X=0; Y= ΔZ, and Z=0; LoS colors represent fields of observation, from surface defined as *Object* to surface *Image* at point (P).

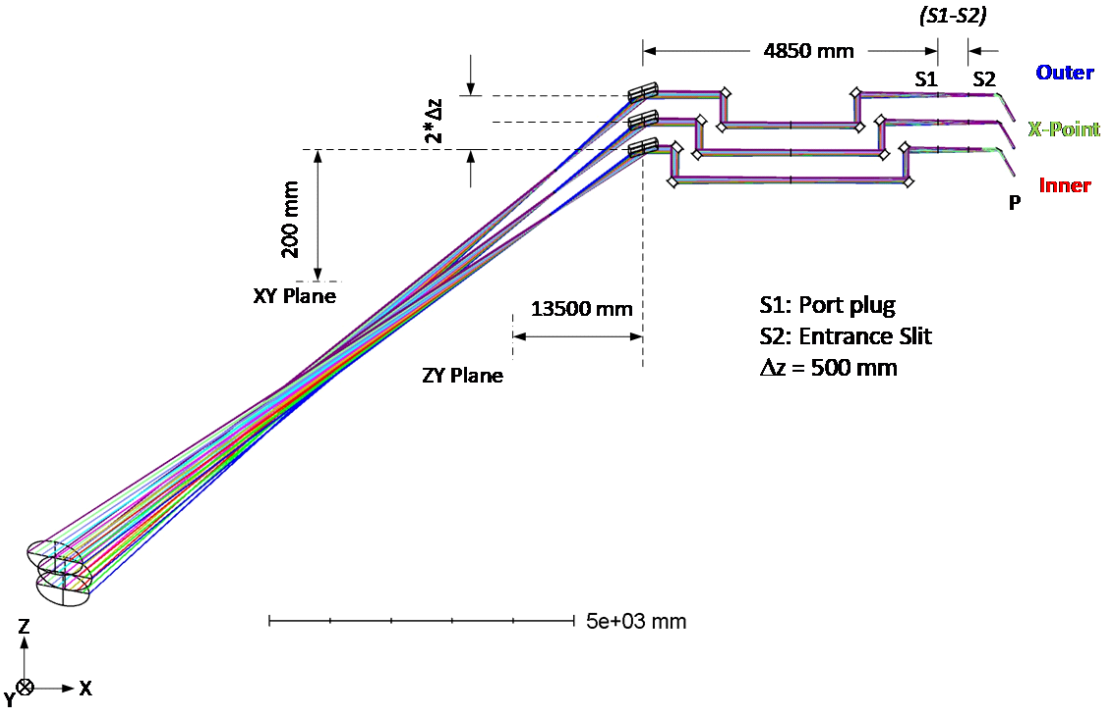

Figure 3: DEMO High-resolution system for plasma divertor parallel observation ZEMAX 3D layout, ZX plane.

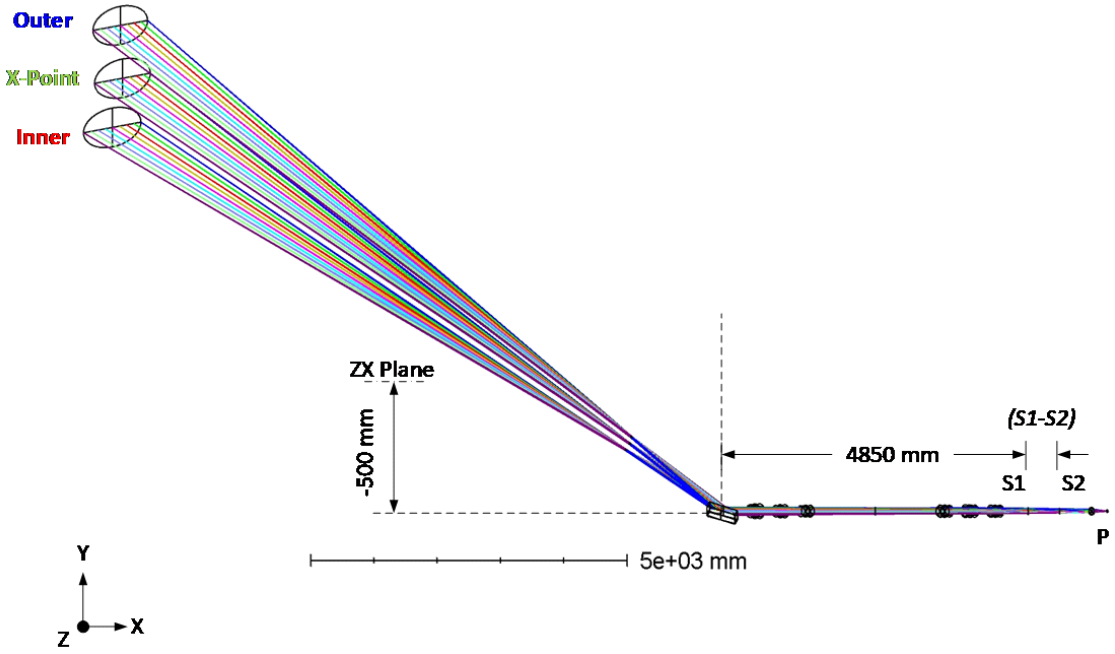

Figure 4: DEMO High-resolution system for plasma divertor parallel observation ZEMAX 3D layout, YX plane.

Single crystal (SC) molybdenum (Mo) and rhodium (Rh) mirrors are considered as the most promising resources for first mirror material due to their good thermal properties, low sputtering yield and good reflectivity in the visible wavelength range [16 -17]; these materials have been defined in ZEMAX and

modeled as coating, considering that any interaction with light occurs primarily within a few nanometers of the surface. The following Table 5, shows the mirror dimensions by subsystem, as a result of the root mean square (RMS) spot radius optimization; considering the tilt angle , see Table 2; the projected length in Z and Y axis are estimated; projected values on Y axis will determine the overall shape and size of the DSM.

Table 5: Results (Mirror dimensions by subsystem)

Target: Outer divertor						
Mirror	M	A	B	C	D	E
Diameter [mm]	223,25	90,21	85,42	91,41	95,36	44,33
Z [mm]	163,94	66,25	62,72	67,12	70,03	32,55
Y [mm]	151,54	61,24	57,98	62,05	64,73	30,09
Target: X-Point						
Mirror	M	A	B	C	D	E
Diameter [mm]	241,21	100,21	90,23	96,03	99,93	55,41
Z [mm]	179,34	74,51	67,09	71,40	74,30	41,20
Y [mm]	161,31	67,01	60,34	64,22	66,83	37,05
Target: Inner divertor						
Mirror	M	A	B	C	D	E
Diameter [mm]	267,34	112,51	98,76	92,22	95,07	65,21
Z [mm]	200,47	84,37	74,06	69,15	71,29	48,90
Y [mm]	176,87	74,43	65,34	61,01	62,90	43,14

The scope of this section concludes with the imaging at the location (P), see Fig 5. Where the footprint diagram displays the beam result of every subsystem superimposed on surface *Image*. This image exhibits a loss of resolution compared to the first approach assumed using only plane mirrors; mirror radii have been optimized from the initial values given in Table 3, achieving a demagnification factor around 20. Rays aberrations and spot analysis offer a wide variety of powerful tools to improve the performance of the system, in terms of resolution and space occupation; issues that will be assessed in subsequent steps of this preliminary design.

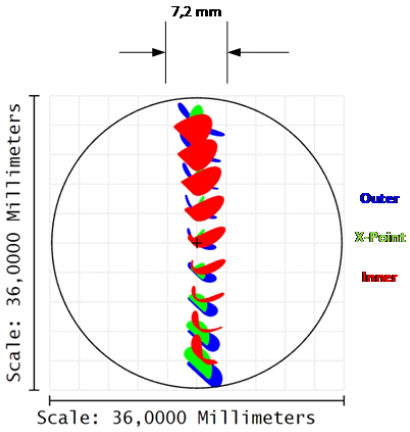

Figure 5: Imaging and footprint spot diagram overview at location (P)

- **ITER–like diagnostic module**

In the previous section, the optical performance is described by the optimization of a ZEMAX RMS spot radius merit function, with a strong constraint dependence on variables that are not yet defined, such as: operation temperature, mechanical tolerances, mirror material and reflectivity; without mentioning the high sensibility to the initial values assumed during the optimization process, and the aberrations introduced by the use of curved mirrors and tilt angles; nevertheless, the numerical assessment of these offer a preliminary idea about the main challenges posed by the conceptual design in terms of feasibility, space required by mirrors, light beam dimensions, shielding scheme and the identification of thermal critical zones. The change of the optical reflectivity of mirror surfaces due to the operation temperature for this case could be omitted; considering that this effect is evidenced for temperatures higher than three-quarters of the melting point, and whose values for Rh and Mo are around 1473C and 1967C respectively; temperatures values that can be controlled via a water cooling circuit, in view of the fact that the power density induced by neutrons on steel at the mirror position expected on DEMO will be less than 1[W/m^3] [15].

A simplified ITER-like diagnostic module has been conceptualized, based on three parameterized labyrinth paths for optics; within a central shield block protected by three ducts with miter bend connections [7] and a lateral common (Cu) cool plate (Thermal sink) to ensure the control on the operation temperature of the mirrors . Fig. 6 shows an overview integration of it on DEMO baseline 2017 model in flat-top plasma scenario [5]; main distances and LoS for divertor parallel observation are indicated as well.

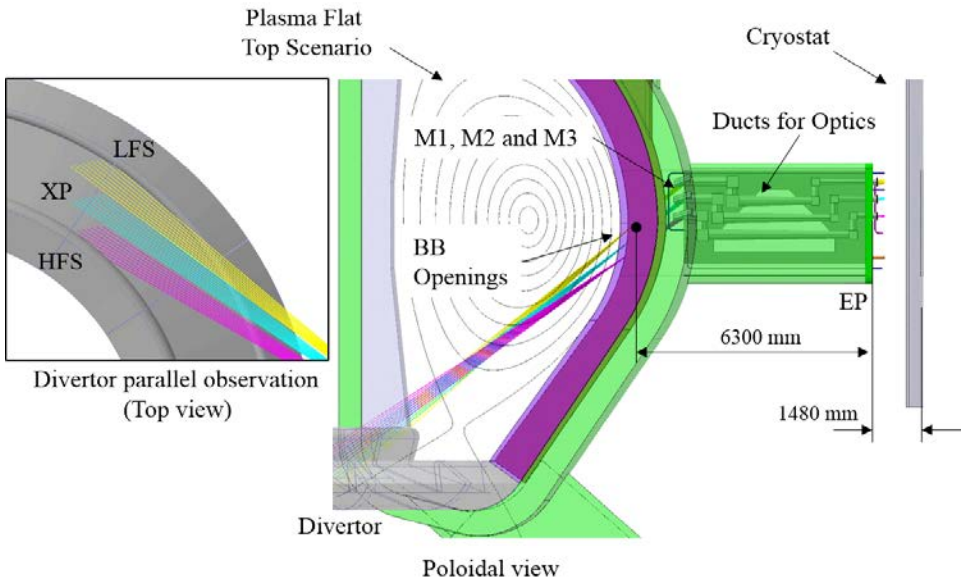

Figure 6: Divertor parallel observation and DSM integration on DEMO baseline 2017.

The diagnostic module integration at EP shows a limited space to host more than two D&C systems with similar dimensions (about 760 mm in width); the idea of a full dedicated EP for divertor plasma control includes the application of a thermography system (outer and inner divertor target) in poloidal orientation, additionally, a core spectroscopy system is foreseen to share the same EP volume. This rough draft is envisaged to be an initial design, aimed to introduce the main R&D critical aspects under a system engineering approach, see Fig. 7.

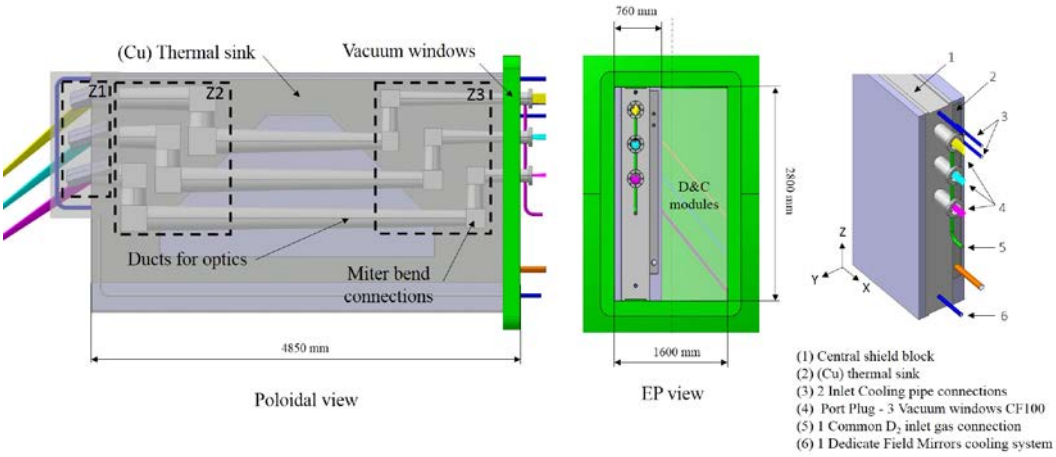

Figure 7: ITER-like module: Poloidal and equatorial port views, space occupation and DSM description.

According to the mirror locations, three areas have been identified as critical for temperature control, where the heat induced by neutrons must be removed effectively to ensure the minimum thermal expansion on mirrors. To this end, two separates cooling circuits have been proposed, the first to provide cooling at the first mirror locations (M1, M2, M3 - Z1), and the second one, to provide cooling at the locations (A, B - Z2) and (C, D - Z3) in parallel. Drops in pressure, mass flow rate and other details are subjects which will be investigated in an advanced stage of design. In addition, an inlet pipe of D_2 gas has been included as an out-vessel connection to supply all the system in parallel, simplifying any possible intervention by remote handling.

- **Conclusions**

Exhaust plasma divertor control represents one of the most important challenges for DEMO D&C; the implementation of a robust high-resolution spectroscopic system for parallel divertor plasma observation has been introduced and a preliminary optical design concept based on plane and toroidal mirrors proposed, aimed to measure the plasma radiation emission in the NUV/VIS range, following the evolution of the enhanced high Balmer line intensities and Stark broadening as indicators of high density plasma (plasma detachment) [1-2]. The system presented for the observation of the whole divertor region is a combination of three parallel imaging optical systems with demagnification factor around 20 in poloidal orientation, protected from neutrons within labyrinth/shielded paths (ducts) with a gas target density $n_G = 3e19m^{-3}$ [8]; the location of the mirrors has been parameterized to simplify and optimize the space required; consequently, imaging simulations have been developed in two steps, initially focusing on the free ray light propagation using planar mirrors and secondly with the intention to reduce the beam dimensions by the inclusion of toroidal mirrors for an intermediate image. Relevant optical dimensions are reported and an ITER-like diagnostic module is proposed.

- **Acknowledgments**

This work has been carried out within the framework of the EUROfusion Consortium and has received funding from the European Union's Horizon 2020 research and innovation programme under grant agreement number 633053. The views and opinions expressed herein do not necessarily reflect those of the European Commission.

References

1. W. Biel et al, *Diagnostic for plasma control – From ITER to DEMO*, Fusion. Eng. Des. (2019) In Press. https://doi.org/10.1016/j.fusengdes.2018.12.092
2.

3. A.G. Meigs et al., *Deuterium Balmer/Stark spectroscopy and impurity profiles: first results from mirror-link divertor spectroscopy system on the JET ITER-like wall*, J. Nucl. Mat, 438 (2013) S607 – S611
4.
5. B.L. Welch et al., *Density measurements in the edge, divertor and X-point regions of Alcator C-Mod from Balmer series emission* , Phys. Plasma 2, 4246 (1995)
6.
7. S. Salasca et al., *The ITER Equatorial Visible/Infra-Red Wide Angle Viewing System: Status of design and R&D*, Fus. Eng. Des, 96-97 (2015) 392-937
8.
9. G. Federici et al., *Overview of EU DEMO design and R&D activities*, Fus. Eng. Des. 89 (2014) 882-889
10.
11. W. Biel et al, *DEMO diagnostics and burn control*, Fus. Eng. Des. 96-97 (2015) 8-15
12.
13. A. J. H. Donné, *Diagnostics for plasma control on DEMO: challenges of implementation,* Nucl. Fus. 52 (2012) 074015 7pp

1. M.Z. Tokar, *Assessment for erosion of and impurity deposition on first mirrors in a fusion reactor*, Nucl. Fusion 58, (2018) 096002
2.
3. G.F Matthews, *Plasma detachment from divertor targets and limiters*, Journal of nuclear materials 220-222 (1995) 104-116
4.
5. W. Gonzalez et al., *Conceptual studies on optical diagnostic systems for plasma control on DEMO,* Fusion. Eng. Des. (2019) In Press. https://doi.org/10.1016/j.fusengdes.2019.03.176
6.
7. V Kotov et al., *Passive protection of the ITER diagnostic mirrors*, Phys. Scr. T145 (2011) 014071 (4pp)
8.
9. A.Lopes, et al., *Neutronics analysis of the ITER Collective Thomson Scattering system,* Fusion. Eng. Des. 134 (2018) 22-28
10.
11. G. Vayakis et al., *Generic diagnostic issues for a burning plasma experiment*, Fus. Sci. and Technology Vol 53, 2018 Issue 2 Pages 699-750

1. K. Ujihara., *Reflectivity of Metals at high Temperatures*, Journal of Applied Physics 43, 2376 (1972)
2.
3. U. Fischer, et al., *Neutronic performance issues of the breading blanket options for the European DEMO fusion power plant*, Fus. Eng. Des. 1019-111 (2016) 1458-1463.
4.
5. J. Peng, et al., *Sputtering tests of single crystal molybdenum and rhodium mirrors at high ion fluence for in situ plasma cleaning of first mirrors in ITER*, Fus. Eng. Des. 128 (2018) 107-112
6.
7. L. Marot et al., *Rhodium coated mirrors deposited by magnetron sputtering for fusion applicatiosn*, Rev. Sci. Inst. 78, 103507 (2007)

1.